Preprint typeset using LaTeX style emulateapj v. 11/12/01

THE LOW-MASS INITIAL MASS FUNCTION OF THE FIELD POPULATION IN THE LARGE MAGELLANIC CLOUD WITH *HUBBLE SPACE TELESCOPE* WFPC2 OBSERVATIONS

D. GOULIERMIS, W. BRANDNER, TH. HENNING
Max-Planck-Institut für Astronomie, Königstuhl 17, D-69117 Heidelberg, Germany
dgoulier@mpia.de, brandner@mpia.de, henning@mpia.de

ABSTRACT

We present V- and I-equivalent HST/WFPC2 stellar photometry of an area in the Large Magellanic Cloud (LMC), located on the western edge of the bar of the galaxy, which accounts for the general background field of its inner disk. The WFPC2 observations reach magnitudes as faint as V = 25 mag, and the large sample of more than 80,000 stars allows us to determine in detail the Present-Day Mass Function (PDMF) of the detected main-sequence stars, which is identical to the Initial Mass Function (IMF) for masses $M \lesssim 1\,M_{\odot}$. The low-mass main-sequence mass function of the LMC field is found *not to have a uniform slope throughout the observed mass range, i.e. the slope does not follow a single power law*. This slope changes at about 1 $M_{\odot}$ to become more shallow for stars with smaller masses down to the lowest observed mass of $\sim 0.7\,M_{\odot}$, *giving clear indications of flattening for even smaller masses*. We verified statistically that for stars with $M \lesssim 1\,M_{\odot}$ the IMF has a slope Γ around –2, with an indicative slope $\Gamma \simeq -1.4$ for $0.7 \lesssim M/M_{\odot} \lesssim 0.9$, while for more massive stars the main-sequence mass function becomes much steeper with $\Gamma \simeq -5$. The main-sequence luminosity function (LF) of the observed field is in very good agreement with the Galactic LF as it was previously found. Taking into account several assumptions concerning evolutionary effects, which should have changed through time the stellar content of the observed field, we reconstruct qualitatively its IMF for the whole observed mass range ($0.7 \lesssim M/M_{\odot} \lesssim 2.3$) and we find that the number of observed evolved stars is not large enough to have affected significantly the form of the IMF, which thus is found almost identical to the observed PDMF.

Subject headings: Magellanic Clouds — galaxies: stellar content — color-magnitude diagrams — stars: evolution — stars: luminosity function, mass function

1. INTRODUCTION

The stellar *Initial Mass Function* (IMF) of a stellar system is a quantity, which accounts for the distribution of the masses of stars assumed to be physically related to each other (as members of the system). This implies that this function is a physical quantity directly linked to the formation of the specific stellar system. Authors refer to the space outside the areas covered by stellar systems, or other stellar structures (such as complexes or aggregates) in a galaxy, as the *field* of this galaxy. The IMF in clustered regions in our galaxy, is found to be about the same as in the solar neighborhood, and also roughly the same as the summed IMF in whole galaxies. So, it is reasonable to assume that most stars form in clusters and not in the general field and that stars in a field region are not necessarily physically related to each other. Hence, in the case of the stellar mass function of the field of a galaxy, we do not necessarily measure a physical quantity of a uniform sample of stars (e.g. with common origin), but rather a distribution of a random sample of stars found in this area under different physical or statistical circumstances (e.g. evaporation from star clusters, dissipation of open clusters, etc).

Although the IMF appears relatively uniform when averaged over whole clusters or large regions of galaxies (Chabrier 2003), observed local spatial variations suggest that they may have statistical origins (e.g. Elmegreen 1999) or that there may be different physical processes working in different mass regimes (e.g. Elmegreen 2004). Indeed, the measured Galactic IMF shows variations of its slope from one region to the other, which could not only reflect sampling limitations in the observations, but they may also be the result of physical differences, or purely statistical in nature. Scalo (1998) notes that while the average slope of the IMF at intermediate to high mass is about the value found originally by Salpeter (1955), i.e., $\Gamma = -1.35$ for stellar counting in equal logarithmic intervals, the slopes for individual regions vary by ± 0.5. It is still unknown if these variations result from physical differences in the intrinsic IMFs for each region, or from statistical fluctuations around a universal IMF. For example in the case of the Orion association, Brown (1998), using Hipparcos data to determine membership, and photometry to determine masses, found an IMF slope of $\Gamma \simeq -1.8$, while a slope fairly consistent with Salpeter's is found by Massey and collaborators for high mass stars in most associations in the LMC and the Milky Way, using spectroscopy to determine masses (e.g. Massey 1998).

The Galactic IMF is found to be approximately a power law for intermediate- to high-mass stars, but it becomes flat at the low-mass regime (Reid 1998), down to the limit of detection, which is around 0.1 $M_{\odot}$ or lower (Lada et al. 1998; Scalo 1986, 1998). The stellar mass at the threshold of the flat part is considered as the thermal Jeans mass in the cloud core, M_{J0} (see review by Chabrier 2003). This mass seems to be higher in star-burst regions (e.g. Scalo 1990; Zinnecker 1996; Leitherer 1998), giving a larger proportion of high-mass stars compared to the solar neighborhood. The proportion of high- and low-mass stars seems to differ for Galactic cluster and field populations as well, in the sense that the slope of the local field star IMF is steeper than the slope of the cluster IMF (e.g. Elmegreen 1997, 1998), which is the case for example for intermediate-mass stars in the solar neighborhood (Scalo 1986). The same observation has been made for the remote field of the LMC for stars in the high-mass (Massey et al. 1995) and the low-mass regime (Gouliermis et al. 2005).

Observed variations from one region of the Galaxy to the other in the numbers of low-mass stars and brown dwarfs over

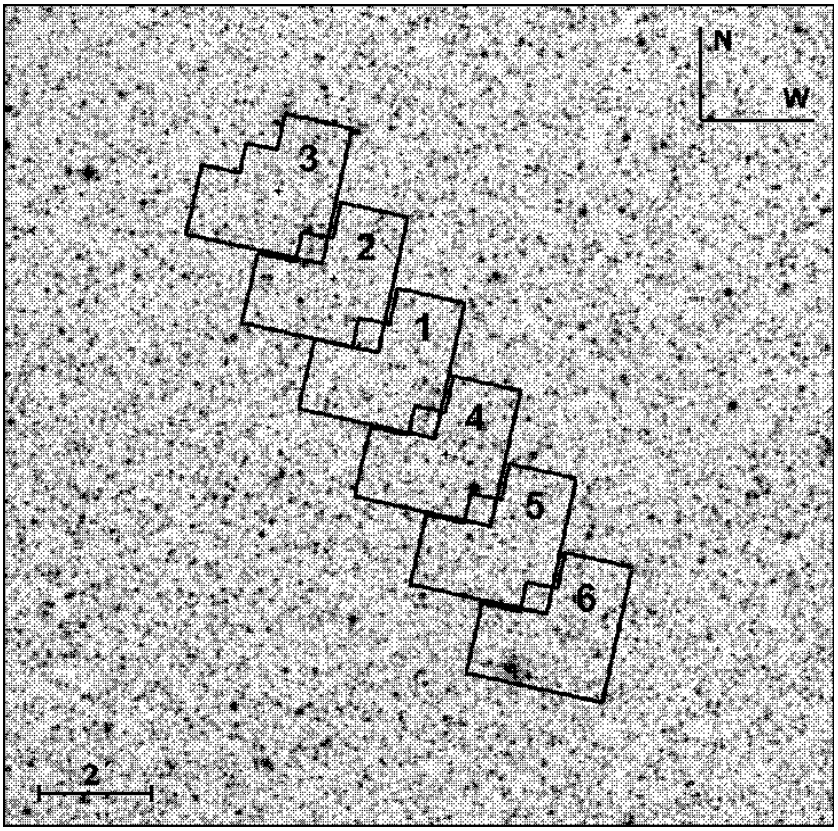

FIG. 1.— The HST/WFPC2 pointings of all six observed datasets. The pointings are overlayed on a $15' \times 15'$ chart of the general area extracted from the SuperCOSMOS Sky Survey. The number of the corresponding dataset is given for every pointing.

the number of intermediate-mass stars affect the corresponding IMF, which seems to depend on the position. In Taurus (Luhman 2000; Briceño et al. 2002) and in IC 348 (Preibisch et al. 2003; Muench et al. 2003; Luhman et al. 2003) the ratio of sub-stellar over stellar objects has been found to be almost half of the value found in the Orion Trapezium cluster (Hillenbrand & Carpenter 2000; Luhman et al. 2000; Muench et al. 2002), in Pleiades (Bouvier et al. 1998; Luhman et al. 2000), in M35 (Barrado y Navascués et al. 2001), and the Galactic field (Reid et al. 1999). Suggested explanations for the low-mass IMF variations include stochasticity in the ages and ejection rates of proto-stars from dense clusters (Reipurth & Clarke 2001; Bate, Bonnell & Bromm 2002; Kroupa & Bouvier 2003), differences in the photoevaporation rate from high-mass neighboring stars (Preibisch et al. 2003; Kroupa & Bouvier 2003), or differences in the initial conditions of the turbulence (Delgado-Donate et al. 2004). They have been also attributed to a dependence of the Jeans mass on column density (Briceño et al. 2002) or Mach number (Padoan & Nordlund 2002), and they may also be affected by variations in the binary fraction (Malkov & Zinnecker 2001). Variations in the IMF have been observed also between different mass ranges within the same region. For example Gouliermis et al. (2005) recently report that the slope of the mass function of a region of a stellar association (LH 52) and a field at the periphery of another association (LH 55 field) in the LMC shows a definite change at about 2 $M_{\odot}$ and it becomes more shallow for higher masses. This is more prominent at the location of the star forming association, which is characterized by a higher number of more massive stars than the field.

Reported variations in the IMF for high mass stars within the same stellar system introduce the phenomenon known as primordial mass segregation, according to which massive stars favor the young cluster cores for birth (e.g. Le Duigou & Knödlseder 2002; Stolte et al. 2002; Sirianni et al. 2002; Muench et al. 2003; Gouliermis et al. 2004; Lyo et al. 2004), while the clusters have not yet the time to be mass segregated by dynamical processes (Bonnell & Davies 1998). This preference of massive stars produce a flattening of the IMF. In a segregated cluster the slope of the massive IMF can be very flat, $\Gamma \sim 0$, while at the cluster envelopes it can be as steep as $\Gamma \sim -2.5$ (de Grijs et al. 2002a). The mechanisms of accretion of peripheral gas (see e.g. Zinnecker 1982; Myers 2000; Larson 2002; Bonnell et al. 2001, 2004; Basu & Jones 2004) and coalescence of other proto-stars in dense cluster cores (Zinnecker 1986; Larson 1990; Price & Podsiadlowski 1995; Stahler et al. 2000; Shadmehri 2004), through which high-mass stars can grow by a much larger factor than low-mass stars, make the IMF depend on environment. Coalescence after accretion drag (Bonnell et al. 1998) or after accretion-induced cloud core contraction (Bonnell & Bate 2002) also seem likely in dense clusters in view of various simulations (Klessen 2001; Bate et al. 2003; Bonnell et al. 2003; Gammie et al. 2003; Li et al. 2004). Furthermore, considering that the confinement of stellar winds and ionization during the collapse phase of massive proto-stars (Garay & Lizano 1999; Yorke & Sonnhalter 2002; Churchwell 2002; McKee & Tan 2003) happens mostly in dense cloud cores, one may expect the massive star formation to be locked to these dense regions. Hence, the flattening of the IMF in dense cluster cores may be partly explained by these

TABLE 1
LOG OF THE OBSERVATIONS. DATASET NAMES REFER TO HST ARCHIVE CATALOG.

Set number	Data Set Name	Filter	Band	Exposure Time (s)	R.A. (J2000.0)	Decl. (J2000.0)
Set 1	U63S010	F555W	WFPC2 *V*	4 × 500	05:01:56	–68:37:20
		F814W	WFPC2 *I*	3 × 700		
Set 2	U63S020	F555W	WFPC2 *V*	4 × 500	05:02:08	–68:35:47
		F814W	WFPC2 *I*	3 × 700		
Set 3	U63S030	F555W	WFPC2 *V*	4 × 500	05:02:20	–68:34:14
		F814W	WFPC2 *I*	3 × 700		
Set 4	U63S040	F555W	WFPC2 *V*	4 × 500	05:01:44	–68:38:53
		F814W	WFPC2 *I*	3 × 700		
Set 5	U63S050	F555W	WFPC2 *V*	4 × 500	05:01:33	–68:40:26
		F814W	WFPC2 *I*	3 × 700		
Set 6	U63S060	F555W	WFPC2 *V*	4 × 500	05:01:21	–68:41:59
		F814W	WFPC2 *I*	3 × 700		

mechanisms, along with dynamical effects (Giersz & Heggie 1996; Gerhard 2000; Kroupa et al. 2001; Portegies-Zwart et al. 2004).

The IMF in the LMC appears to be steep in areas of the general field, away from any stellar system. Massey et al. (1995) found that stars in the LMC field have an IMF slope $\Gamma \sim -4$, the same value as for the Milky Way field (see also Massey 2002). The massive stars inside known Lucke & Hodge (1970) OB associations in the LMC are found to have $\Gamma = -1.08 \pm 0.2$, whereas the dispersed massive stars outside the associations have a bit steeper IMFs with $\Gamma = -1.74 \pm 0.3$ (Hill et al. 1994). This result is in line with Parker et al. (1998) who found that stars not located in HII regions (they refer to them as field stars) have an IMF with $\Gamma \sim -1.8 \pm 0.09$, while the IMF of stars located in HII regions (related to known stellar associations) exhibit possibly three slopes: $\Gamma = -1.0$, -1.6, and -2.0. They interprete this variability of Γ as the result of differing star formation processes.

Gouliermis et al. (2002) make a distinction between a known stellar association in the LMC (LH 95), its surrounding field (located at the periphery of the association) and the general background field of the galaxy (farther away from the system). They found that the IMF of stars with $3 \lesssim M/M_{\odot} \lesssim 10$, in the area of the association has a slope $\Gamma \approx -2$, while in the surrounding and remote fields $\Gamma \approx -3$ and -4, respectively. According to Parker et al. (2001) corrections for field star contamination of the IMFs of associations can reduce an apparent slope Γ from -1.7 to -1.35. Hence, it should be kept in mind that inadequate corrections for background stars may result in a steeper-than-in-reality IMF. Indeed according to Gouliermis et al. (2002) the slope of the field-subtracted IMF of the association LH 95 is found to be $\Gamma \simeq -1.6 \pm 0.3$ for $3 \lesssim M/M_{\odot} \lesssim 10$, which becomes even more shallow with $\Gamma \simeq -1.0 \pm 0.2$ if a wider mass range is taken into account ($3 \lesssim M/M_{\odot} \lesssim 28$). For comparison, Garmany et al. (1982) found $\Gamma = -2.1$ outside the solar circle and $\Gamma = -1.3$ inside, for stars more massive than 20 $M_{\odot}$ within 2.5 kpc of the Sun. Later Casassus et al. (2000) found little difference between the IMF slope inside and outside the solar circle, being steeper than Salpeter's with $\Gamma \sim -2$ everywhere, in line with previous results, according to which the local field IMF is found to have a slope $\Gamma \sim -1.7$ to -1.8 (Scalo 1986; Rana 1987; Kroupa, Tout, & Gilmore 1993). Kroupa & Weidner (2003) suggest that superposition of Salpeter IMFs with a cluster mass function slope of -2.2 explains the $\Gamma \sim -1.8$ field star IMF.

Stellar cluster formation theories for turbulent molecular clouds show that many processes are operating simultaneously, and it may be difficult to find out which particular process dominates during the formation of a particular star cluster. However, these theories consider partitioned IMFs. For example, Bate et al. (2002) have distinguished brown dwarf formation from that of other stars, and Gammie et al. (2003) have shown that the high-mass part of the IMF gets shallower with time as a result of coalescence and enhanced accretion. According to Elmegreen (2004) there is an advantage in viewing the IMF in a multi-component way, because it allows observers to anticipate and recognize slight variations in the IMF for different classes of regions when they are sampled with enough stars to give statistically significant counts. The same author discuss the differences between the IMFs observed for clusters and remote fields and suggests a three-component model of the IMF to consider possible origins for the observed relative variations in brown dwarf, solar-to-intermediate mass, and high-mass populations. He finds that these variations are the result of dynamical effects that depend on environmental density and velocity dispersion. Elmegreen's models accommodate observations ranging from shallow IMF in cluster cores to Salpeter IMF in average clusters and whole galaxies to steeper IMF in remote field regions.

In this study we present an example for the local variations of the slope of the present-day mass function (PDMF or MF) in the general field of the LMC, with high statistical significance, based on HST/WFPC2 observations on six sequential fields located at the inner disk of the galaxy close to the edge of its bar. The observed change of the MF slope is verified statistically and it shows a trend of the MF to become flat for sub-solar masses. Since these stars did not have the time to evolve, the MF in the range $M \lesssim 1\,M_{\odot}$ accounts for the IMF of the LMC field. We reconstruct the IMF of the field for higher masses after correcting for evolutionary effects and we find that the change of the slope at about one solar mass stands also for the LMC field IMF up to about $2.5\,M_{\odot}$.

The outline of this paper is the following: In the next section (§2) we present our data and we describe the performed photometry. The star formation history, as it was defined from

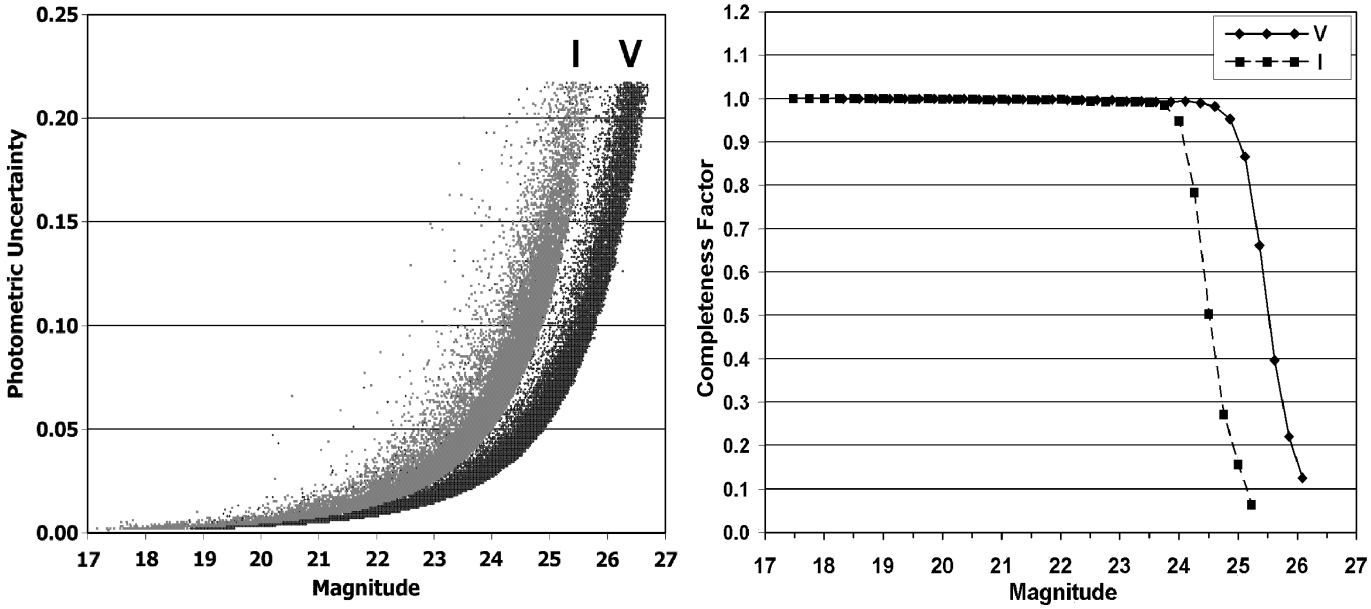

FIG. 2.— Uncertainties of photometry (left) and completeness factors (right) as derived by HSTphot from all six data sets, for both $F555W$ (V) and $F814W$ (I) bands.

previous studies is presented in in §3, where the investigation of the observed populations takes place and the observed color-magnitude diagram (CMD) is presented. The determination and the study of the LF and the MF of the main-sequence stars in the area is described in §4, where we also present the IMF of the general LMC field of the inner disk, as it is reconstructed after several assumptions have been taken into account. General conclusions of this investigation are presented in §5.

2. OBSERVATIONS AND DATA REDUCTION

The studied area is located in the inner disk of the galaxy, very close to the western edge of the bar. The WFPC2 images of this area were collected as target of the *Hubble Space Telescope* program GO-8576. Six sequential telescope pointings were obtained, which cover a line from North-East to South-West. In total the integration time is 2,000 seconds observed in the *F555W* filter ($\sim V$) and 2,100 seconds in *F814W* ($\sim I$) for each pointing. The exposure times are given in Table 1, together with other details of the observations. The WFPC2 fields, overlayed on a SuperCOSMOS Sky Survey image of the general area, are shown in Figure 1. The photometry has been performed using the package HSTphot as developed by Dolphin (2000a). We added the individual exposures in each filter for each field, with the use of the subroutine *coadd*, to construct deep ones. These exposure times cover the high dynamic range of brightness of the stars in the region with good overlap between sets. We compared the long exposures with the shorter ones to check for saturated stars and it seems that the brightest stars are within the observed dynamic range. The detection limit of these observations is at $V \sim 26.5$ mag.

For the data reduction and the photometry we used the most recent version of the HSTphot package (version 1.1.5b; May 2003). This version allows the simultaneous photometry of a set of images obtained by multiple exposures. HSTphot uses a self-consistent treatment of the charge transfer efficiency and zero-point photometric calibrations and it is tailored to handle the under-sampled nature of the point-spread function (PSF) in WFPC2 images (Dolphin 2000b). We followed the standard procedures for removing bad columns and pixels, charge traps and saturated pixels (subroutine *mask*), and for the removal of cosmic rays (subroutine *crmask*) as described by Dolphin (2000a). Since HSTphot allows the use of PSFs which are computed directly to reproduce the shape details of star images as obtained in the different regions of WFPC2, we adopted the PSF fitting option in the photometry subroutine (*hstphot*), instead of performing aperture photometry. Data quality parameters for each detected source are returned from *hstphot*, and we selected the values, which account for the best detected stars in uncrowded fields, as recommended in "*HSTphot User's Guide*" (object type 1 or 2, sharpness between –0.3 and 0.3 and $\chi \leq 2.5$).

HSTphot provides directly charge transfer efficiency corrections and calibrations to the standard VI system (Dolphin 2000b). Figure 2 (left panel) shows typical uncertainties of photometry as a function of the magnitude for the two filters. The completeness of the data was evaluated by artificial star experiments, which were performed for every observed field separately with the use of the HSTPhot utility *hstfake*. The completeness was found not to change at all from one frame to the other. The overall completeness functions are shown in Figure 2 (right panel) for both filters. The chip of WFPC2 consists of four frames, one of which (PC frame) has double resolution but half field-of-view than the remaining three (WF frames). Our artificial-stars test showed that the completeness within the PC frame of each camera pointing is somewhat lower than the one of the WF frames. We noticed that this phenomenon is related to the small numbers of detected stars in the PC frames, which are smaller than the ones of the corresponding WF frames of the neighboring pointings, which overplot them. Consequently, for this study we make use of the stars found only in the WF frames of the six observed WFPC2 fields, which provide us with better number statistics.

3. STELLAR POPULATIONS IN THE LMC FIELD

The area investigated here accounts for the background field population of the LMC inner disk close to the western edge of

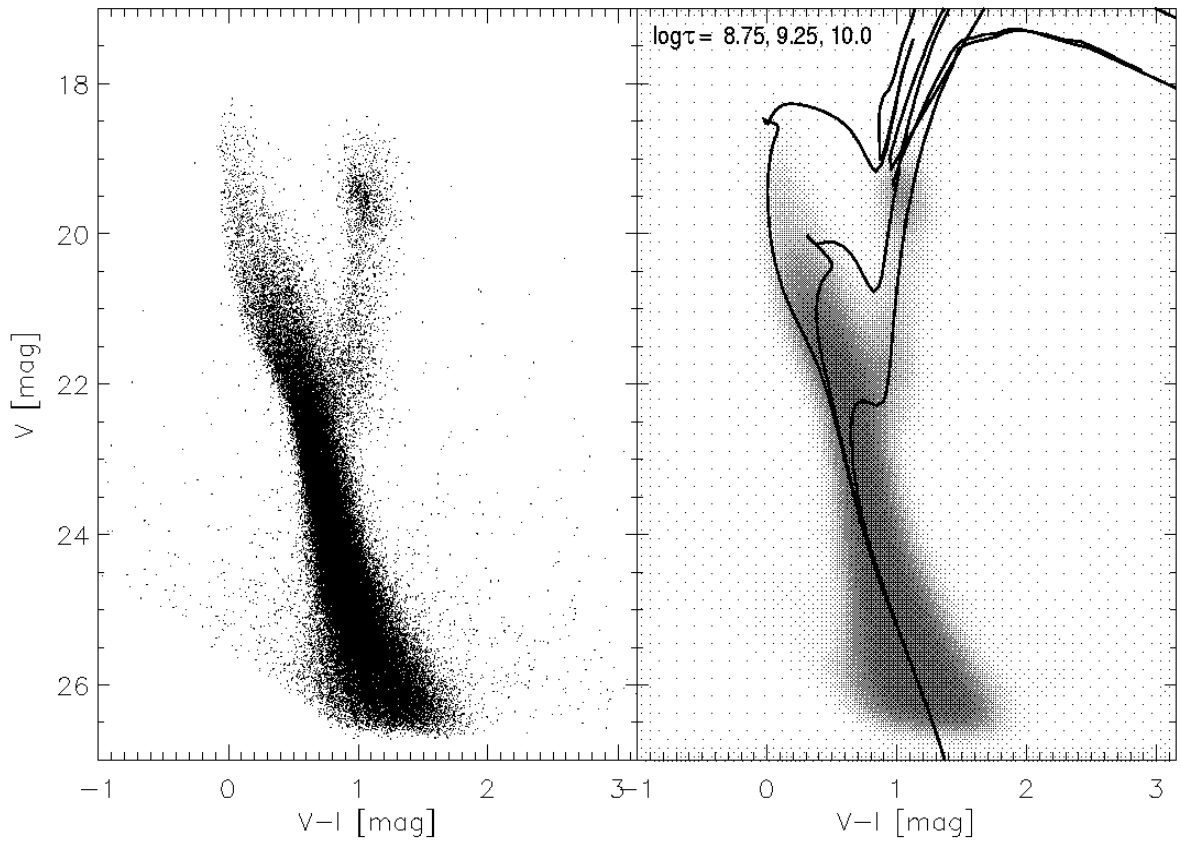

FIG. 3.— Left: $V-I$, V Color-Magnitude Diagram (CMD) of the stars in all six observed WFPC2 fields. Right: Smoothed CMD of the same stars with reddened isochrone models from Padova group overplotted.

the bar of the galaxy. We performed star counts on the stellar catalog of every one of the six observed frames, to check for any stellar overdensity, which would be expected in case of a concentration of stars, and would be an indication of the existence of a stellar system. There are a few stellar clumps, of which none shows a stellar density higher than 3σ over the background density (where σ is the fluctuation in stellar density). The observed area is checked with SIMBAD for known stellar systems and only one is found, which is located at the south-eastern part of pointing No. 6 (Figure 1), and which has been identified as a star cluster by Kontizas et al. (1990; KMHK 448), but it has not been revealed with a stellar density higher than 3σ in our observations. Consequently there is no indication of the co-existence of different stellar populations in the observed area, which thus can be considered to be representative as a whole of the field population of the inner disk of the LMC.

3.1. *Star Formation History of the LMC*

The general background field of the LMC has been previously observed with HST/WFPC2 by several authors. These studies, having concentrated on the star formation history (SFH) of the galaxy, give consistent results. The first such investigation is by Gallagher et al. (1996), who observed a field at the outer disk of the LMC, while a field in the inner disk of the galaxy was observed by Elson et al. (1997). Three fields of the outer disk were studied by Geha et al. (1998). Two of those fields are also presented by Holtzman et al. (1999) with an additional field located in the LMC bar. More recently, Castro et al. (2001) observed seven additional fields, all located at the outer disk. Smecker-Hane et al. (2002) studied a field at the center of the LMC bar and another one in the inner disk. The most recent investigation, which makes use of such data is by Javiel et al. (2005), who use the same data material as Castro et al., to present an analysis of the SFH of the LMC. These studies cover the whole sample of investigations on the SFH of the galaxy with HST/WFPC2 observations, and they cover a sample of 14 WFPC2 fields, which are spread in a large area of the LMC, from the center of the bar to the edge of the outer disk.

The results of these investigators of the SFH in the disk (outer/inner) and the bar of the LMC will be summarized in the following: In general the LMC field is dominated by an old stellar population with $\tau \gtrsim 10$ Gyr (Castro et al. 2001). A major increase in the star formation rate (SFR) occurred ~ 2 Gyr ago, which resulted in almost 25% of the field stellar population, including much of the LMC disk (Gallagher et al. 1996). Elson et al. (1997) found that an intense star formation event, which occurred ~ 2 - 4 Gyr ago, probably corresponds to the formation of the disk. An increase (by a factor of 3) of the SFR, almost 2 Gyr ago, was also suggested by Geha et al. (1998). According to the same authors a closed-box chemical evolution scenario implies that the LMC metallicity has been doubled the past 2 Gyr. Events of enhanced SF are found to have taken place in the north, north-west regions of the disk 2 - 4 Gyr ago also by Castro et al. (2001). Javiel et al. (2005) using the same observational material found slightly earlier events of enhanced SF at

1 to 2 or 3 Gyr ago for the north-western regions, located at the outer LMC disk. The SFH of the LMC disk seems to have remained continuous with almost constant SFR over the last ~ 10 Gyr (Geha et al. 1998) or 15 Gyr (Smecker-Hane et al. 2002). The bar of the LMC has been found to contain a larger number of older stars than in the disk (Holtzman et al. 1999) and according to Smecker-Hane et al. (2002) it probably formed during an episode that occurred 4 - 6 Gyr ago. These authors also suggest that both the bar and disk of the LMC experienced similar SFHs at ~ 7.5 to 15 Gyr. It is worth noting that active SF during the past ~ 0.1 - 1 Gyr was also found in the disk by Gallagher et al. (1996). The conclusive results presented here on the SFH of the galaxy will provide a baseline for the interpretation of the features observed in the color-magnitude diagram of the area, presented in the next section.

3.2. *Color-Magnitude Diagrams*

Each of the observed WFPC2 fields includes around 13,500 stars. Hence the overall stellar catalog, which includes almost 80,000 stars, provides a rich sample of the LMC disk population. The $V-I$ vs. V Color-Magnitude diagram (CMD) of these stars is shown in Figure 3 (left panel). As can be seen from this CMD the LMC field is characterized by a prominent red-giant clump located around $V \simeq 19.5$ mag and $(V-I) \simeq 1.1$ mag, and a large number of low-mass MS stars below the turn-off point of the ~ 10 Gyr model. These features are also apparent in the CMDs presented in the investigations of the SFH of the LMC, mentioned above. Furthermore, there is a lack of main-sequence stars brighter than $V \sim 18$ mag in all CMDs. We verified that in our fields this is not because of saturation. Indeed, the LMC field is known to have only a few massive MS stars per unit area (Massey et al. 1995). The similarity of the CMDs of all these various WFPC2 fields suggests that the stellar content of the general LMC field does not change significantly from one area to the next, although the SFH of the bar has been found to be somewhat different to the one of the disk of the galaxy, as we discussed above. However, our fields are only in the disk and not in the bar.

There are also variations in the stellar density of the LMC field between different areas. These variations are found to be due to a gradient in the number of stars, with higher numbers towards the center of the galaxy (Castro et al. 2001). Each of the areas observed by Smecker-Hane et al. (2002) in the bar and the inner disk of the galaxy ($1.^\circ7$ southwest of the center of the LMC) covers $\simeq 10^5$ stars, which correspond to about 15,000 stars per WFPC2 field. These stellar numbers are in agreement with the ones of the fields presented here and observed within the same HST proposal ($\sim$ 13,500 stars per WFPC2 field) and the $\sim$ 15,800 stars observed by Elson et al. (1997) in another WFPC2 field at the inner disk. On the other hand each of the WFPC2 fields at the outer disk studied by Castro et al. (2001) contains around 2,000 stars in agreement with the number of detected stars by Gallagher et al. (1996) in their single field, which is also located in the outer disk. The number of stars in the general LMC field found in one WFPC2 field earlier by us (Gouliermis et al. 2005; $\sim$ 4,000 stars) is in line with these variations, since this field is not close to the bar, but still much closer to it than all the previously mentioned outer disk fields.

Concerning the SFH of the area presented here, the information provided in the previous section is more than sufficient for the age distribution of the contributing populations in the CMD of Figure 3 to be accurately estimated. In the same figure (right panel) we present a smoothed image of the CMD with three indicative isochrone models overplotted. The models of the Padova group in the HST/WFPC2 magnitude system (Girardi et al. 2002) were used. These isochrone fits indeed show that the stellar populations of the area seem to be the product of star formation events that took place 0.5 - 3 Gyr ago. In addition, the sub-giant region of the CMD is very well traced by models of older ages ($\gtrsim$ 10 Gyr). It should be noted that according to the tabulation by Ratnatunga & Bahcall (1985), the contamination of the CMD by Galactic foreground stars is expected to be negligible. Furthermore, the investigation of Metcalfe et al. (2001) on the Hubble Deep Fields, has shown that also the number of background faint galaxies in such a CMD, is very small for stars brighter than V $\simeq$ 25 mag.

Isochrone fitting showed that the color excess toward every one of the six observed fields is almost the same and it can be considered as uniform for the whole area. The mean value of the color excess from isochrone fitting was found to be $E(V-I) \simeq 0.05$, which corresponds to $E(B-V) \simeq 0.03$ (e.g. Rieke & Lebofsky 1985). The reddening curve R_V (ratio of the total absorption in V, A_V, to $E(B-V)$), has been found to be consistent by various authors (Mihalas & Binney 1981: R_V = 3.2; Koornneef 1983: R_V = 3.1; Leitherer & Wolf 1984: $R_V \simeq 3.13$). Adopting the value estimated by Taylor (1986; R_V = 3.15), the absorption toward this area is $A_V \simeq 0.095$ mag. The models in Figure 3 are reddened accordingly. We adopted the distance modulus for the LMC derived by Panagia et al. (1991) from SN 1987A, 18.5 ± 0.1 mag, which corresponds to a distance of 50.1 ± 3.1 kpc.

4. LUMINOSITY AND MASS FUNCTION OF THE FIELD

4.1. *Luminosity Function*

We examine the main-sequence luminosity function (LF) of the stars found in all six observed fields (overall catalog). We constructed the LF of the stars based on the WF frames of the WFPC2 fields only, due to their better completeness, as mentioned earlier. The main-sequence stars were selected according to their positions in the CMD and their LF, Φ, was constructed by counting them in magnitude bins and normalizing their numbers to the same surface of 1 kpc^2. The constructed LF is shown in Figure 4 (left panel). The solid line represents the LF uncorrected for completeness. The completeness corrected LF is plotted with thick dots. As shown by the completeness functions of Figure 2, the stellar sample down to $V \simeq 25$ mag is complete by 95% (which corresponds to $I \simeq 24$ mag). Then the completeness falls rapidly to almost 50% within 0.5 magnitudes. The steep decline of the completeness for stars fainter than $V \simeq 25$ mag introduces the sharp rise of the completeness-corrected LF toward the faint end. Since only data within the 50% completeness limit can be used this rise affects only the last three useful magnitude bins (the arrow in Figure 4 indicates the 50% completeness limit).

The comparison of this LF with the ones presented by Smecker-Hane et al. (2002) of their "Disk 1" field and the bar region shows that these LFs are similar to each other in various aspects. Specifically, in the LF of Figure 4 one can observe a change of its slope at $V \sim 22.2$ - 22.4 mag, like in both bar and disk LFs of Smecker-Hane et al. (2002). This magnitude corresponds to the turn-off for stars of age ~ 2 Gyr and this change is much smoother than in the case of Smecker-Hane et al. LFs. In addition, we observe changes in the slope of our LF, which seem to coincide with two of the three "spikes" (as Smecker-

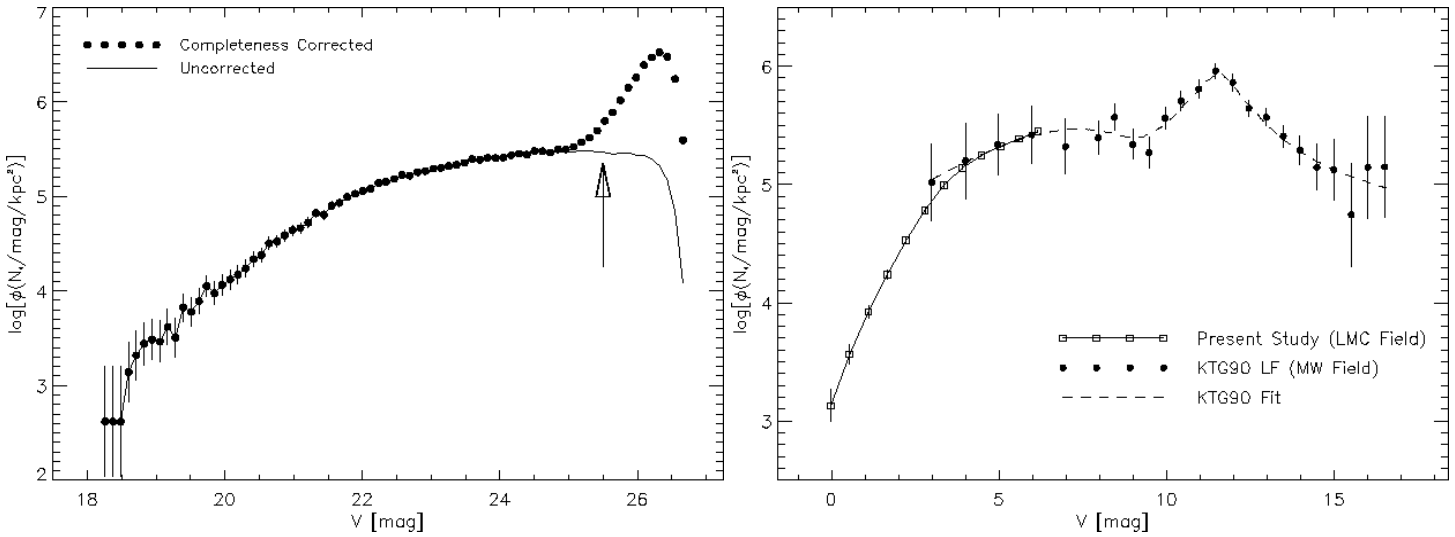

FIG. 4.— Left: Main-sequence Luminosity Function of the stars in all six observed fields. The arrow indicates the 50% completeness level. Right: Comparison between the LF for the stars in the LMC field observed in this study within the 80% completeness limit (open points) and the one for field stars near the Sun from Scalo (1989) and Stobie et al. (1989) (filled points) together with the corresponding smooth fit (dashed line) adopted by Kroupa et al. (1990; KTG90). It is interesting to note that our LF for the low-mass stars is in very good agreement with the LF of the solar neighborhood in their region of overlap.

Hane et al. call them) observed in the bar LF at almost the same magnitudes ($V \simeq 19.6$ and 20.4 mag). This shows that the LF of our area, which belongs to the inner disk, is more similar to the one of the bar than of the outer disk. This is more or less expected, considering that our area is close to the edge of the bar (0.°3 away), while the "Disk-1" field of Smecker-Hane et al. (2002) is located almost at the edge of the inner disk, about 1.°5 away from the bar.

It is worthwhile to compare our LF with the one of low-mass field stars in the solar neighborhood, as it is constructed with data taken from Stobie et al. (1989) (for $M_V > 7$ mag) and Scalo (1989) ($7 \geq M_V/\mathrm{mag} \geq 3$). To do so we resample our data into wider bins, and we construct the LF of our LMC field with a sampling similar to the one of the solar neighborhood LF, as it is presented by Kroupa et al. (1990). This comparison, which is shown in Figure 4 (right panel) shows that the LF of the low-luminosity stars seems to be the same between the LMC general field and the local field of the Milky Way for $2.5 \lesssim M_V/\mathrm{mag} \lesssim 6.5$. This magnitude range covers the brighter part of the flattening of the local neighborhood LF, which corresponds to absolute magnitude $M_V \sim +7$ mag and which is the result of effects of H^- molecules on the opacity and equation of state (Kroupa et al. 1990). These effects together with the ones of H_2 and other molecules introduce points of inflexion in the mass-luminosity relation, at which the dominant opacity source in the stellar atmosphere changes rapidly. The solar neighborhood LF of Figure 4 has a maximum near $M_V \sim 12$ mag, which according to Kroupa et al. (1990) is consistent with being a consequence of a point of inflexion in the mass-luminosity relation, caused by the effect of H_2 on stellar photosphere. Our data do not allow us to compare these LFs toward fainter magnitudes.

4.2. *Mass Function*

4.2.1. *Fundamental Definitions*

The distribution of stellar masses calculated for a given volume of space in a stellar system is known as the Present Day Mass Function (PDMF), which we usually call the Mass Function of the system. In the case of the area presented here, there is no specific stellar system to which the observed stars seem to belong and the distribution of their masses represents the PDMF of the field population of the inner LMC disk. We will refer to the function $\xi(\log m)$, which gives the number of stars per unit logarithmic (base ten) mass interval $d\log m$ per unit area (e.g. /kpc^2) as the *mass function* (MF) of the field. This function usually replaces the *mass spectrum* $f(m)$, which is the number of stars per unit mass interval dm per unit area. The characterization of these functions is based on the various parameterizations used for the Initial Mass Function (IMF) of a stellar system (see e.g. Kroupa 2002). Very useful parameters are the indices of the mass spectrum $f(m)$, and of the mass function $\xi(\log m)$, defined as

$$\gamma = \frac{d\log f(m)}{d\log m} \tag{1}$$

and

$$\Gamma = \frac{d\log \xi(\log m)}{d\log m} \tag{2}$$

These are the logarithmic slopes of $f(m)$ and $\xi(\log m)$ and for power-law mass spectra they are independent of mass (Scalo 1986). A reference slope is the logarithmic derivative $\Gamma = -1.35$, which is the index of the classical IMF for stars in the solar neighborhood with masses $0.4 \lesssim M/M_\odot \lesssim 10$, found by Salpeter (1955). The corresponding mass spectrum has $\gamma = \Gamma - 1 \simeq -2.35$. The lognormal field star IMF fit by Miller & Scalo (1979) has $\Gamma \simeq -(1+\log m)$. A basic relation between $\xi(\log m)$ and $f(m)$ is $\xi(\log m) = (\ln 10)\cdot m \cdot f(m) \simeq 2.3 \cdot m f(m)$ (see Scalo 1986).

4.2.2. *Construction of the Mass Function*

In the present study we construct the MF $\xi(\log m)$ by counting stars in logarithmic (base ten) mass intervals. The counting of stars in mass intervals can be achieved by translating their luminosities (or magnitudes) into masses using mass-luminosity relations and then constructing the distribution of the derived masses. This method is definitely dependent on the adopted evolutionary models used for the transformation of luminosities to masses. de Grijs et al. (2002b), who presented a thorough investigation of the Mass-Luminosity (M/L) relation found that

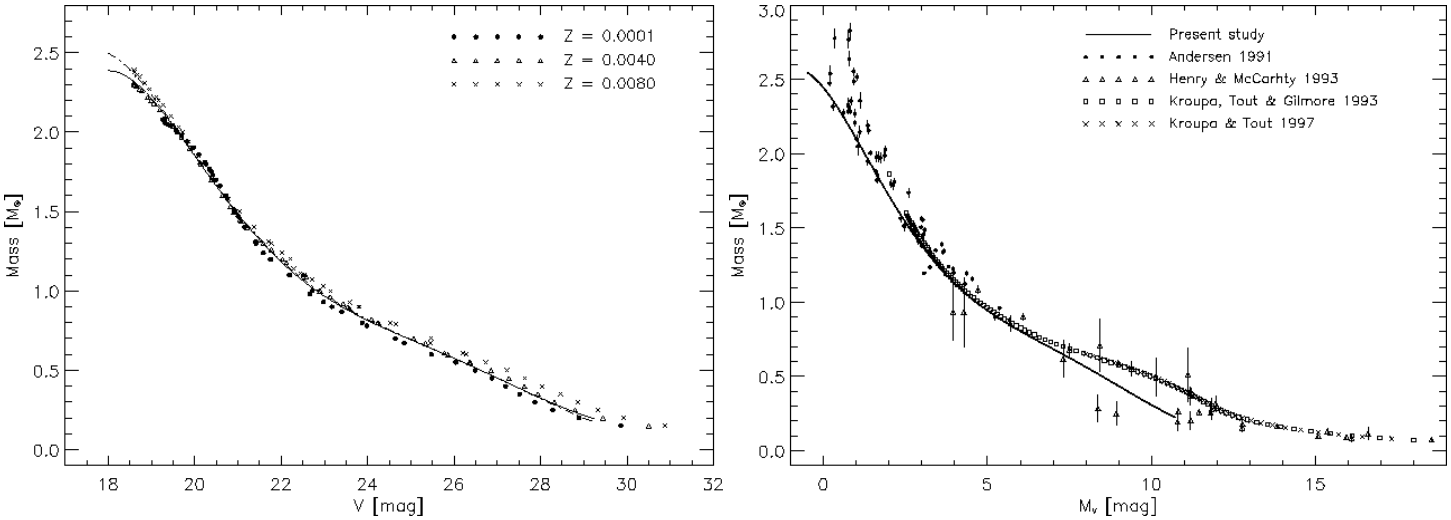

FIG. 5.— Left: Mass-to-Luminosity Relation, constructed in this study according to three isochrone models and for three assumed metallicities. Right: Comparison of this relation, adopted here, with previous empirical and semi-empirical relations.

this model dependence results only in a systematic offset of the overall masses.

For the determination of the M/L relation we used the latest Padova theoretical isochrones in the HST/WFPC2 Vega system (Girardi et al. 2002). These models were originally developed by Girardi et al. (2000) and they were transformed to the HST/WFPC2 pass-bands as described in Salasnich et al. (2000). The M/L relation of our study here is defined by the models of three different ages. These models (overplotted over the CMD in Figure 3 - right panel) are carefully selected as the most representative of the age limits estimated for the observed field population. These limits, which have been verified by previous investigations of the SFH of the general LMC field population (see §3.1), cover an age span between $\sim$ 0.6 - 10 Gyr ($8.75 \lesssim \log\tau \lesssim 10$). The M/L relation for the main-sequence stars in the observed CMD was developed according to the main-sequence part of the evolutionary models. For the low main-sequence population the 10 Gyr model provided the M/L relation for stars up to $M_{\rm V} \simeq 6.95$ mag ($0.7\,M_{\odot}$). A model, which corresponds to a median age ($\sim$ 1.8 Gyr) was used for the M/L relation for stars with magnitudes from $M_{\rm V} \simeq 6.97$ mag ($0.7\,M_{\odot}$ according to this model) up to $M_{\rm V} \simeq 3.8$ mag ($\sim 1.1\,M_{\odot}$).

For the upper main-sequence stars in the observed fields, which correspond to the younger population, the 0.6 Gyr model was used. The use of any younger isochrone would have no meaning, because there are no stars in the CMD of Figure 3 brighter than the turn-off of the 0.6 Gyr model, also considering that there are no saturated stars in any observed field. Therefore, the highest mass that could be measured from these data according to the $\sim$ 0.6 Gyr isochrone is $\lesssim 2.5\,M_{\odot}$ (which corresponds to $M_{\rm V} \simeq 0.06$ mag). In all models the LMC metallicity of Z = 0.008 was taken into account. This value is in the range of values $0.002 < {\rm Z} < 0.018$ compiled by Kontizas et al. (1993) from the literature. In order to check for any biases in the determination of the M/L relation due to an adopted wrong metallicity, the procedure described above was repeated also for models of lower metallicities (Z=0.004 and Z=0.0001). We found that there are *no significant differences between the derived M/L relations from models of different metallicities.* This is shown in Figure 5 (left panel), where the relation of magnitudes and masses for each model has been plotted. Three different symbols represent the M/L relations derived from models of different metallicity. The corresponding polynomial fits on the data for Z=0.008 (dashed line) and on all the data (solid line) are overplotted. These fits differ slightly only at the higher mass by $0.1\,M_{\odot}$. The overall polynomial fit (solid line) is the adopted M/L relation for the construction of the MF of the LMC field in this study.

This fit is plotted in Figure 5 (right panel), along with M/L relations derived from previous empirical (Andersen 1991; Henry & McCarthy 1993) and semi-empirical (Kroupa et al. 1993; Kroupa & Tout 1997) studies for solar-metallicity stellar populations for $M \lesssim 2\,M_{\odot}$. For solar metallicities in the mass range $0.1 < M/M_{\odot} \lesssim 1$ Kroupa & Tout (1997) conclude that the theoretical M/L relations of Baraffe et al. (1995) provide the best overall agreement with all recent observational constraints. Their semi-empirical M/L relation though (plotted in the right panel of Figure 5), is closely followed by the theoretical M/L solar abundance relation by Chabrier et al. (1996) (see also de Grijs et al. 2002b). The best match with the observational data for low-metallicity Galactic globular clusters for masses $M \lesssim$ 0.6 - 0.8 $M_{\odot}$ is found by Piotto et al. (1997) to be provided by the theoretical M/L relations of Alexander et al. (1997). The comparison of our M/L relation based on the Padova models with the previous studies shows a very good agreement for the magnitude range of interest ($M_{\rm V} \lesssim 6.5$ mag), although there is a small difference toward the bright end of the plot (for $0 \lesssim M_{\rm V}/{\rm mag} \lesssim 2.5$). In addition there is a slight offset of our fit toward smaller masses.

Here we have a final comment on the constructed M/L relation and the resulting MF. We checked both the present-day and initial stellar masses of each magnitude as they are provided by the models and we found that they are exactly the same for stars with magnitudes within the limits covered by the part of the main-sequence of each model used for the construction of our M/L relation. This fact implies that evolutionary effects did not reduce the stellar masses through mass loss. Consequently all used mass bins for the construction of the MF correspond to both the present-day and initial stellar masses. This will be useful later for the reconstruction of the IMF of these stars.

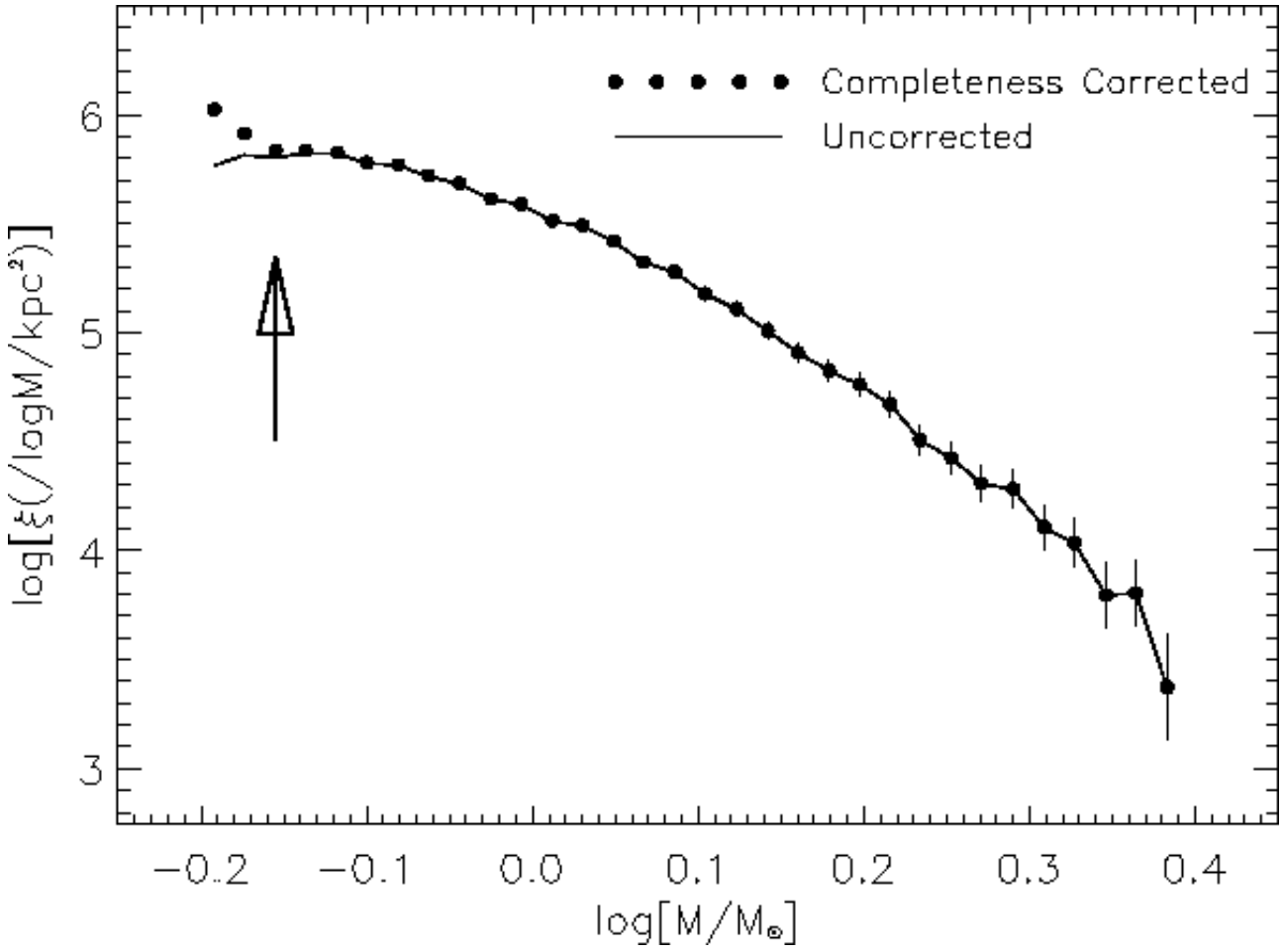

FIG. 6.— Main-sequence Mass Function of the stars detected in the WF frames of all six observed fields, for completeness $\gtrsim$ 50%. The arrow indicates the $\sim$ 95% completeness limit.

4.2.3. *Linear Regression*

The constructed MF of the main-sequence stars in the observed fields is shown in Figure 6. The stars were counted in logarithmic mass intervals according to their masses as they were estimated with the use of the M/L relation presented in the previous section. The stellar numbers are normalized to a surface of 1 kpc^2. In Figure 6 the MF not corrected for incompleteness is represented by a line, and points indicate the corrected MF. Only data within 50% of completeness are plotted and the arrow indicates the $\sim$ 95% completeness limit.

The very fine binning in this MF gives the impression that this distribution cannot be considered as a unique power-law throughout its whole mass range. Indeed, it seems that there is a gradual change in the slope of the MF similar to the one observed in the LF (see §4.1). In order to check for variations in the slope of the MF for stars in different mass ranges we modeled the MF data with a weighted linear fit (*linear regression*). Specifically, we considered the problem of fitting a set of N data points ($\log m_i$, $\log\xi(\log m_i)$) to a straight-line model

$$\log\xi(\log m) = \Gamma\cdot\log m + \beta \qquad (3)$$

considering different ranges of mass bins ($\log m_i$) from the MF shown in Figure 6. For simplicity we call the function $F(m) = \xi(\log m)$. Hence Equation (3) becomes

$$\log F(m) = \Gamma\cdot\log m + \beta. \qquad (4)$$

The fit was applied for the data up to the highest available mass bin of $M \simeq 2.4\ M_\odot$, but each time changing the considered low-mass bin, down to the one, which corresponds to 50% completeness ($M \simeq 0.63\ M_\odot$). For every considered mass range we evaluated the MF slope Γ and we measured how well the model agrees with the data using the chi-square merit function (Press et al. 1992), which in this case is

$$\chi^2(\beta,\Gamma) = \sum_{i=1}^{N}\left(\frac{\log F_i - \beta - \Gamma\cdot\log m_i}{\sigma_i}\right)^2 \qquad (5)$$

where σ_i is the uncertainty associated with each measurement F_i. We are interested to find the mass range within which the linear model of Equation (4) is in the best agreement with the data. Hence we estimated for every mass range the goodness-of-fit of the data to the model, which is the probability Q that a value of χ^2 as poor as the value in Equation (5) should occur by chance, given by the equation:

$$Q = \mathcal{G}\left(\frac{N-2}{2}, \frac{\chi^2}{2}\right) \qquad (6)$$

where $\mathcal{G}$ is the incomplete gamma function $Q(\beta,\log m)$. The goodness-of-fit is believable if Q is larger than about 0.1, while for $0.001 \lesssim Q \lesssim 0.1$, the fit may be acceptable if the errors are non normal (Press et al. 1992).

TABLE 2

SLOPES Γ OF THE MF AND THE CORRESPONDING GOODNESS-OF-FIT (Q) FOR THE LINEAR REGRESSION (LEAST χ^2 METHOD) FOR DIFFERENT MASS INTERVALS. WITH THE APPLICATION OF LINEAR REGRESSION FOR DIFFERENT MASS RANGES WE FOUND THAT THE MF SLOPE SHOWS A STATISTICALLY SIGNIFICANT CHANGE AT ABOUT 1 $M_\odot$. THE ROWS MARKED WITH BOLDFACE CHARACTERS INDICATE THE MASS RANGE AT WHICH THE FIT STARTS TO GIVE BELIEVABLE RESULTS ($Q \gtrsim 0.1$).

Mass Range ($M_\odot$)	N	Γ	β	Q
0.64 - 2.42	32	-2.91 ± 0.04	9.04 ± 0.00	0.000
0.67 - 2.42	31	-2.94 ± 0.04	9.04 ± 0.00	0.000
.	.	.	.	.
.	.	.	.	.
.	.	.	.	.
0.94 - 2.42	23	-4.23 ± 0.09	9.14 ± 0.01	0.000
0.98 - 2.42	22	-4.43 ± 0.10	9.16 ± 0.01	0.011
1.03 - 2.42	**21**	$\mathbf{-4.59 \pm 0.11}$	$\mathbf{9.19 \pm 0.01}$	**0.087**
1.07 - 2.42	20	-4.79 ± 0.12	9.22 ± 0.02	0.678
1.12 - 2.42	19	-4.90 ± 0.14	9.24 ± 0.02	0.781
1.17 - 2.42	18	-4.99 ± 0.16	9.26 ± 0.02	0.816
1.22 - 2.42	17	-5.17 ± 0.18	9.29 ± 0.03	0.963
1.27 - 2.42	16	-5.23 ± 0.21	9.31 ± 0.04	0.953
.	.	.	.	.
.	.	.	.	.
.	.	.	.	.
0.64 - 1.03	12	-2.13 ± 0.07	9.13 ± 0.01	0.000
0.67 - 1.03	11	-1.88 ± 0.08	9.14 ± 0.01	0.000
0.70 - 1.03	10	-1.87 ± 0.10	9.14 ± 0.01	0.003
0.73 - 1.03	**9**	$\mathbf{-2.08 \pm 0.12}$	$\mathbf{9.13 \pm 0.01}$	**0.117**
0.76 - 1.03	8	-2.27 ± 0.14	9.12 ± 0.01	0.390
0.79 - 1.03	7	-2.36 ± 0.18	9.12 ± 0.01	0.356
0.83 - 1.03	6	-2.64 ± 0.23	9.11 ± 0.01	0.782
.	.	.	.	.
.	.	.	.	.
.	.	.	.	.

NOTE: The mass of $\sim 0.64\ M_\odot$ represents the 50% completeness limit, and the 95% completeness limit corresponds to $\sim 0.70\ M_\odot$.

4.2.4. *Results for the Mass Function*

With this procedure we found that, for data within the 50% completeness, not the whole observed mass range shows a significant correlation between the mass and the corresponding stellar numbers (both in logarithmic scale). In Table 2, the results of the linear regression for selected samples are shown. It is found that an acceptable linear correlation between $\log F(m)$ and $\log m$ ($Q \gtrsim 0.1$) starts to appear for stars within mass ranges with a lower limit $M \simeq 1.0\ M_\odot$. From this limit on and for mass ranges with lower limits of higher masses the goodness-of-fit becomes continuously higher, showing a better linear correlation. The highest mass limit used is $M \simeq 2.4\ M_\odot$.

The next step is to repeat this procedure in order to define the mass range with the best linear correlation for stars with masses smaller than the limit of $\sim 1.0\ M_\odot$. We found that the data are very well linearly correlated for masses in the range starting at $\simeq 0.73\ M_\odot$ and higher (second set of slopes in Table 2). The MF slope in this mass range ($0.73 \lesssim M/M_\odot \lesssim 1.03$) is $\Gamma \simeq -2.1 \pm 0.1$ (steeper than Salpeter's IMF), in contrast to the slope for masses $1.0 \lesssim M/M_\odot \lesssim 2.4$, which is found to be steeper with $\Gamma \simeq -4.6 \pm 0.1$. We used as lower mass limit $0.7\ M_\odot$, which corresponds to the completeness limit of 95%, to perform an additional test. It should be noted that for smaller masses the completeness falls rapidly (see §2), so that the completeness corrections introduce a very steep distribution of the very low-mass data (as shown in the LF of Figure 4), which does not have necessarily any physical meaning. Consequently, we do not consider the MF with $M < 0.7\ M_\odot$ test.

Hence, considering the fixed lower-mass limit to be $0.7\ M_\odot$, we performed the same procedure for smaller mass intervals and found that intervals, which correspond to continuously smaller masses have a MF slope, which changes gradually to become almost Salpeter's value ($\Gamma \simeq -1.4$ for $0.7 \lesssim M/M_\odot \lesssim 0.9$) or even more shallow. The estimated slopes are given in Table 3, which demonstrates that the MF toward the smaller observed masses becomes flat. Unfortunately, this result for the shorter mass ranges is based on small numbers of bins, and thus on poor number statistics (last rows in Table 3). A turn-over of the MF cannot be observed, unless deeper data with better completeness are used. This result, which is a clear indication of a low-mass flattening of the MF, also indicates that the estimated MF slope is very sensitive to the selected mass range.

TABLE 3

SLOPES Γ OF THE MAIN-SEQUENCE MF FOR THE LINEAR FITS FOR DIFFERENT MASS RANGES, WITH LOWER MASS LIMIT AT $0.7\,M_{\odot}$. IT IS SHOWN THAT THE MF SLOPE IS BECOMING GRADUALLY MORE SHALLOW FOR SMALLER MASS INTERVALS TOWARD THE LOW-MASS OBSERVABLE LIMIT WITHIN THE 95% COMPLETENESS. THE BOLDFACE ROW INDICATES AGAIN THE MASS RANGE AT WHICH THE FIT STARTS TO BE BELIEVABLE.

Mass Range ($M_{\odot}$)	N	Γ	β	Q
.	.	.	.	.
.	.	.	.	.
.	.	.	.	.
0.70 - 1.12	12	-2.03 ± 0.08	9.13 ± 0.01	0.00
0.70 - 1.07	11	-1.94 ± 0.09	9.14 ± 0.01	0.00
0.70 - 1.03	10	-1.87 ± 0.10	9.14 ± 0.01	0.00
0.70 - 0.98	9	-1.72 ± 0.11	9.16 ± 0.01	0.02
0.70 - 0.94	8	-1.63 ± 0.13	9.17 ± 0.01	0.03
0.70 - 0.90	**7**	$\mathbf{-1.40 \pm 0.16}$	$\mathbf{9.20 \pm 0.02}$	**0.23**
0.70 - 0.86	6	-1.25 ± 0.19	9.22 ± 0.02	0.27
0.70 - 0.83	5	-1.01 ± 0.25	9.25 ± 0.03	0.41
0.70 - 0.79	4	-0.94 ± 0.35	9.26 ± 0.05	0.25
0.70 - 0.76	3	-0.27 ± 0.54	9.35 ± 0.07	0.78

NOTE: The mass of $\sim 0.70\,M_{\odot}$ represents the 95% completeness limit.

Taking into account that stars of small masses evolve very slowly one may assume that the low-mass MF has a slope close to Salpeter's because it actually accounts for the Initial Mass Function (IMF) of these stars, and that the steepening of the higher mass MF is due to evolutionary effects. We investigate this aspect in the next section, where we also attempt a reconstruction of the IMF of the observed LMC field in a qualitative manner, taking several assumptions into account.

5. RECONSTRUCTION OF THE INITIAL MASS FUNCTION

In this section we use the information on the (present-day) MF of the LMC field in the observed area, to reconstruct its IMF. In order to achieve this we have to make a number of assumptions concerning the evolution process of the stars found in the area. An issue to be clarified first is *if the present-day mass, as it was estimated from the models for each main-sequence star, differs from the corresponding initial mass*. Considering that for stars in the observed mass range no mass loss takes place we checked the models and we verified that indeed for each magnitude bin used for the construction of the adopted M/L relation, *the present-day stellar masses are exactly equal to their initial values for the main-sequence stars*. This was verified for the models of all three considered metallicities and for the mass ranges, for which each one of the three adopted ages was used ($0.2 \lesssim M/M_{\odot} \lesssim 0.7$ for $\tau \simeq 10$ Gyr, $0.5 \lesssim M/M_{\odot} \lesssim 1$ for $\tau \simeq 2$ Gyr and $1 \lesssim M/M_{\odot} \lesssim 2.4$ for $\tau \simeq 560$ Myr).

Consequently, the masses estimated for the observed main-sequence stars, which were used for the construction of their PDMF are actually the initial masses of the stars (without taking the red giants into account) and thus, they correspond also to their IMF. If mass-loss would occur, as is the case for high-mass stars, then the present-day masses of the stars would not be useful for the construction of their IMF, because the stars would be distributed in mass bins different than those of their original masses. Since this is not the case, the expected differences between the PDMF and the IMF of the observed main-sequence stars are mostly due to different stellar numbers and not due to different mass estimates, which would redistribute the same stars in different mass bins. It should be noted that the observed MF of the lower main-sequence stars, below a specific turn-off, which did not have the time to evolve, should account for the IMF of these stars. We discuss this in the following section.

5.1. *Assumptions concerning the small masses*

The first assumption that has to be made for the reconstruction of the IMF considers the upper mass limit of the *lower main-sequence* stars. Specifically, is should be defined which stars actually belong to the "lower main-sequence". A reasonable assumption is to define this upper mass limit as the turn-off (MSTO) of the 10 Gyr isochrone. The choice of this isochrone is based on the fact that this model seems to represent the majority of the sub-giant branch shown in Figure 3. Below this magnitude there should be also primordial faint main-sequence stars, but an examination of both the MSTO of the 10 Gyr model and the one of the oldest available of 15.5 Gyr showed that they do not differ significantly. Specifically the two MSTOs differ by almost 0.4 magnitudes, the brighter point being the value for the younger isochrone of course, which accounts for $0.1\,M_{\odot}$. The (initial) mass of the MSTO for the 15.5 Gyr model is around $0.85\,M_{\odot}$, and for the 10 Gyr is about $0.95\,M_{\odot}$. Hence, we can safely state that *the observed PDMF accounts for the IMF of stars with masses up to* $\simeq 0.9\,M_{\odot}$.

It should be noted that while the exact details of the star formation history (SFH) of the LMC are still under debate, various authors suggest that the $\gtrsim$ 12 Gyr old population does not contribute more than $\approx 5\%$ to the total low-mass stellar content of the LMC, and that the past 2 to ≈ 7 Gyr saw several epochs with strongly enhanced star formation rates (see, e.g, Gallagher

et al. 1996; Elson et al. 1997; Geha et al. 1998). A 5% contribution of $\gtrsim$ 12 Gyr old stars to the stellar population should only have a minor effect on the overall slope of the present day mass function. Hence we suggest that the observed flattening of the PDMF towards lower masses is an intrinsic feature of the LMC IMF. A more definitive statement regarding the LMC IMF, however, can only be obtained once the LMC SFH has been derived in an unambiguous way.

As far as the younger stellar population, which is also located at this part of the CMD, is concerned we compared the values of the initial masses, corresponding to the same magnitudes in the old ($\tau \gtrsim$ 10 Gyr), the intermediate (2 $\lesssim \tau$/Gyr $\lesssim$ 10), and the young (0.5 $\lesssim \tau$/Gyr $\lesssim$ 2) isochrone models, and we found that the larger differences in the initial mass of the faint main-sequence stars appear toward the brighter limits. These differences do not account for more than $\sim 0.1\ M_{\odot}$, and they are extremely small toward the fainter magnitudes. Consequently the most age-sensitive mass bins of the constructed MF are the ones between 0.9 and 1 $M_{\odot}$. Since the MF shown in Figure 6 has a mean mass bin width of 0.03 $M_{\odot}$, the 10% differences in the mass estimation of individual stars can account for up to three mass bins, and consequently may change the MF slope as it is estimated, by redistributing stars in neighboring bins.

In order to check if this is the case we constructed the MF of the area using wider bins ($\sim 0.1\ M_{\odot}$), and we applied again a linear regression to estimate the MF slopes in different mass intervals and to check for any significant changes in the MF. Of course for this MF we were able to verify these differences with coarser uncertainties, because of the use of wider bins. The χ^2 test showed that indeed there is a linear correlation between $\log F(m)$ and $\log m$, which appears for the mass range from the higher mass bin ($\sim 2.4\ M_{\odot}$) down to $\sim 1\ M_{\odot}$. According to the same test there is no linear correlation at all for wider mass ranges. The MF slopes were found to be comparable to the ones estimated for the MF of narrower binning for almost the same mass range.

In general, with the tests above and the construction of a MF with wider bins we were able to verify that the use of a unique M/L relation does not affect the estimated MF slopes significantly. Consequently, we can safely conclude that *the coexistence of low-mass stars of different age at the lower part of the main sequence does not affect the corresponding MF slope up to $\sim$ 0.9 - 1 $M_{\odot}$*. Under these circumstances the MF of the main-sequence stars, shown in Figure 6, represents their IMF for masses up to this mass limit.

5.2. *Assumptions concerning the larger masses*

As far as the upper main-sequence is concerned, i.e. main-sequence stars with $M \gtrsim 0.9\ M_{\odot}$, although their estimated masses are almost equal to their initial masses according to the models, their numbers per mass bin do not trace directly the IMF, because of the existence of evolved stars, which should be taken into account. A smooth and continuous star formation rate in the LMC (e.g. Smecker-Hane et al. 2002) would naturally lead to a PDMF with a progressively steepening slope towards higher masses. While all primordial stars with masses $\lesssim 0.9\ M_{\odot}$ are still present on the main-sequence, the most massive stars successively evolve off the main-sequence with increasing age of a stellar population. As these stars ultimately end up either as black holes, neutron stars, or white dwarfs, the optical data presented in this paper could not account for them in any comprehensive way and in the following discussion we consider only the red giants and white dwarfs (WDs).

Stars of mass comparable to that of the Sun evolve to form white dwarfs, while above some critical mass, $M_{\rm c}$, they explode as Type II supernovae instead. Predictions for $M_{\rm c}$ range from 6 to 10 $M_{\odot}$, depending on the models (Weidemann 1990; Jeffries 1997; García-Berro et al. 1997; Pols et al. 1998). Elson et al. (1998) have identified a candidate luminous white dwarf with an age of 12×10^5 yr in NGC 1818, a young star cluster in the LMC with HST/WFPC2 observations. This discovery constrains the boundary mass for WDs in the LMC to $M_{\rm c} \gtrsim 7.6\ M_{\odot}$. Models also suggest that WDs should have $(V-I) \sim -0.4$ mag (e.g. Wood 1991; Cheselka et al. 1993), a value which is roughly independent of age and metallicity. For the WFPC2 passbands $F555W$ and $F814W$ this color is equivalent to $(V-I) = -0.44$ mag (Holtzman et al. 1995), and thus the range of colors in which we might expect to find WDs in the CMD of Figure 3 is $-0.64 \lesssim (V-I)/\mathrm{mag} \lesssim -0.24$ (Elson et al. 1998). This gives roughly 25 candidate WDs (not corrected for completeness), almost half of which have magnitudes $V \lesssim$ 24.5 mag, while the rest are very close to the detection limit and can be spurious detections as well. This very small number leads to the conclusion that the contribution of WDs to the IMF of our fields should be negligible.

Therefore, in order to correct the MF for evolutionary effects we consider the existence of red giants only, and we make use of their initial mass per magnitude provided by the Padova models, assuming that no nova or super-nova explosion occurred in the observed field. A simple assumption that can be made is that few old isochrones are sufficient for the estimation of the masses of the observed RGB stars shown in the CMD of Figure 3. Although, the stellar masses according to the isochrone models do not differ significantly from one model to the next on the main-sequence, this is not the case for the red-giant branch. Specifically, the mass provided by the 10 Gyr model for a typical LMC metallicity (Z = 0.008) for RGB stars with -1 $\lesssim M_{\rm V} \lesssim$ 4 is between 0.97 and 0.99 $M_{\odot}$, while the model for $\sim$ 2 Gyr gives masses $1.59 \lesssim M/M_{\odot} \lesssim 1.66$ for the same magnitude range. On the other hand metallicity does not seem to affect significantly the resulting masses. For example, the corresponding masses from models of the same age for lower metallicity (Z = 0.0001) are 0.86 - 0.87 for 10 Gyr and 1.42 - 1.44 for 2 Gyr. Consequently, in order to establish a realistic representation of the IMF of our RGB stars, a careful selection of the models for the estimation of their initial masses should be made.

This selection is based on the results on the SFH of the LMC, discussed earlier (§3.1). These results can be summarized as a major increase in the SFR occurring about 2 - 4 Gyr ago (Elson et al. 1997; Castro et al. 2001) and according to other authors about 2 Gyr ago (Gallagher et al. 1996; Geha et al. 1998; Smecker-Hane et al. 2002; Javiel et al. 2005). Gallagher et al. (1996) suggest that this later enhancement in the SFR resulted in 25% of the field population, while Smecker-Hane et al. (2002) found that the increase in the SFR 1 - 2 Gyr ago produced 15% of the stellar mass in the bar. Taking these numbers into account it would be reasonable to assume that 20% of the RGB population was formed around 2 Gyr ago. Furthermore, considering that 25% of the stars in the bar were probably formed about 4 - 6 Gyr ago (Smecker-Hane et al. 2002), we can assume that 25% of the RGB population in our CMD has an age of about 5 Gyr. Finally, since the LMC field population is dominated mostly by stars of age $\sim$ 10 Gyr (Castro et al. 2001), the

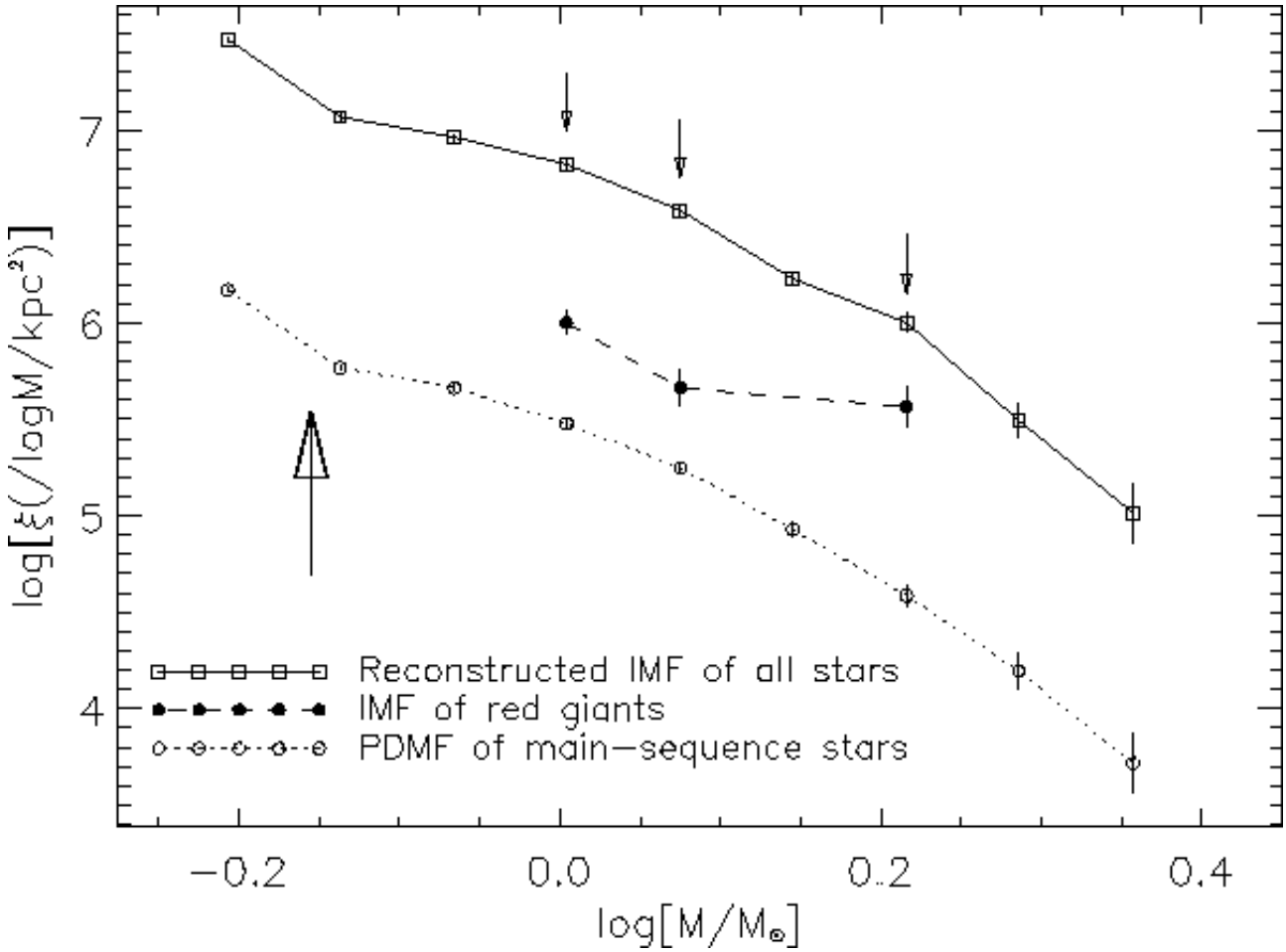

FIG. 7.— The Initial Mass Function of all stars in the observed area (red giants and main-sequence), as it is reconstructed under the assumptions discussed in §5, plotted with box symbols and the solid line. The small number of RGB stars in the area and their narrow mass range introduce only small changes in three specific mass intervals of the main-sequence MF (small arrows), showing only a trend of the IMF to become slightly more shallow toward the limit of $\sim 1.6\,M_{\odot}$. The red-giants IMF has been constructed by counting stars in coarser mass intervals, because of the small number statistics for the red giants, and it is plotted with solid dots and dashed line. The main-sequence MF of Figure 6 constructed with the same binning is also plotted, with open dots and dotted line. All mass functions shown are shifted to avoid overlapping. The large arrow indicates the 95% limit of completeness.

model of this age should be used for the rest of our RGB stars. Ultimately, the Padova isochrone model of ~ 2 Gyr for 20% of the RGB stellar population, the one of ~ 5 Gyr for 25% of the population and the model for 10 Gyr for 55% of the population will be used for the estimation of their initial masses and the construction of the red-giant IMF of our sample.

Taking all the above hypotheses into account for the reconstruction of the IMF of the observed area, the resulting IMF may be considered as a rough representation of the IMF of the LMC field at the edge of its bar, and as the most realistic as possible, within the uncertainties caused by our assumptions. According to the models used for the estimation of the masses of the red giants in our sample, these stars fall in few very narrow mass ranges, not allowing the construction of their IMF with the fine binning of the main-sequence MF shown in Figure 6. Thus, we counted all red giants in wider logarithmic mass intervals, which resulted in only three bins for their IMF, which are plotted in Figure 7 (thick dots - dashed line). We constructed the main-sequence MF with the same grosser binning and we also show it in Figure 7 for comparison (open dots - dotted line). The small numbers of bins in the red-giant IMF only provides a qualitative estimate of the IMF.

From Figure 7 it can be seen that the slope of the red-giant IMF tends to be more shallow than the main-sequence MF for the same mass range ($1 \lesssim M/M_{\odot} \lesssim 1.6$). This trend is also present in the IMF of the whole population, which is shown as it was constructed with the use of the same binning (Figure 7), making it a bit more shallow for the same mass range (the affected bins are indicated by the small arrows in the figure). Still, the small number of RG in our sample compared to the MS population (~ 1900 red giants to $\sim 75{,}000$ stars selected as main-sequence stars), cannot change significantly the slope of the MF already shown in Figure 6. If this tentative result represents reality then *the IMF of the LMC field in the observed area does not differ much from its present-day MF for the mass range* $0.7 \lesssim M/M_{\odot} \lesssim 2.4$.

6. CONCLUSIONS AND DISCUSSION

We made use of a large sample of almost 80,000 stars observed with HST/WFPC2 in a region of about 32 arcmin^2 in the general field west of the bar of the LMC to construct its main-sequence PDMF and, based on several assumptions, to qualitatively reconstruct its IMF. The conclusions of this study can be summarized as: (1) *The main-sequence LF of the observed LMC field is in very good agreement with the Galactic LF* as it was previously found (Kroupa et al. 1990) within the overlap-

ping magnitude range of $3 \lesssim V/\mathrm{mag} \lesssim 6$. (2) We verified statistically that in the observed area *the main-sequence MF of the LMC field does not follow a single power law*, but it changes at about 1.0 $M_\odot$ to being shallower for stars with smaller masses down to the lower observed mass (within 95% completeness) of about 0.7 $M_\odot$. (3) The main-sequence PDMF of stars with masses between $\sim 0.9\,M_\odot$ and $0.7\,M_\odot$ is found well correlated with mass with a slope Γ starting from −1.4, comparable to Salpeter's IMF, to become flatter for shorter mass ranges (Table 3). This provides a clear hint of flattening of the main-sequence MF of the LMC field below $\sim 0.7\,M_\odot$. This MF accounts for the IMF of the LMC field in the low-mass regime. The IMF becomes very flat with $\Gamma \approx -0.3$ for the lowest observed masses (within the 95% completeness), but this result is based only on three mass bins, and thus suffers from poor statistics. Deeper observations would certainly provide a larger number of stars in this mass range and thus more information on the low-mass flattening of the LMC field IMF. (4) The slope of the main-sequence MF becomes a bit steeper for masses higher than $\sim$ 0.9 up to $\sim 1\,M_\odot$ (–2.9 $\lesssim \Gamma \lesssim$ –2.7). For masses between $\sim 1\,M_\odot$ and the highest observed mass ($\sim 2.3\,M_\odot$) it is even steeper with $-5.2 \lesssim \Gamma \lesssim -4.5$, similar to the one previously found in the same mass range (Gouliermis et al. 2005), and for massive stars (Massey et al. 1995). (5) We attempted a qualitative reconstruction of the IMF in the whole observed mass range $0.7 \lesssim M/M_\odot \lesssim 2.3$.

A comparison between the IMF in clustered star-forming regions of low and high density environments (e.g. Hill et al. 1994; Hill et al. 1995) shows that there are systematic differences in the IMF from one stellar system to the next in the LMC. However, Massey & Hunter (1998) found that the IMF slope in R136 in 30 Doradus is indistinguishable from those of Galactic and Magellanic Cloud OB associations and they suggest that star formation produces the same distribution of masses over a range of ~ 200 times in stellar density, from that of sparse OB associations to that typical of globular clusters. Indeed the IMF slopes of LMC associations are found by various authors (Massey et al. 1989a,b, 1995; Parker et al. 1992; Garmany et al. 1994; Oey & Massey 1995; Oey 1996; Dolphin & Hunter 1998; Parker et al. 2001; Olsen et al. 2001; Gouliermis et al. 2002) are similar, considering the observational constraints, and are clustered around $\Gamma \approx -1.5 \pm 0.1$ for intermediate-to-high-mass stars. This slope is not very different from the mass function slopes of typical LMC clusters for the same mass range (e.g. Hunter et al. 1997; Fischer et al. 1998; Grebel & Chu 2000; de Grijs et al. 2002; Gouliermis et al. 2004). In general, if the observed differences from cluster to cluster are subject to systematic uncertainties, or if the small fluctuations around a typical Salpeter IMF are related to the density of the regions is still unknown.

On the other hand the observed difference between the LMC field high-mass star IMF (e.g. Massey et al. 1995; Parker et al. 1998), which has a slope around $\Gamma \simeq -4$, and the IMFs found for stellar associations in this galaxy (see references above) is larger than the measured uncertainties, and thus it cannot be accounted entirely to observational constraints in the detection of low-mass stars. Furthermore, Gouliermis et al. (2005) recently showed that the field of the LMC is characterized by the majority of the observed stars with $M < 2\,M_\odot$ with an IMF slope $\Gamma \approx -5$. Such a difference of the IMF slope has been also observed in the solar neighborhood (Scalo 1986; Tsujimoto et al. 1997), but in this case corrections for low and intermediate masses, such as the loss of evolved stars and possible variations in the past star formation rate should be taken into account (Scalo 1986). Consequently, the solar neighborhood field may be considered as a composite of several different cluster IMFs from aging dispersed loose stellar systems and thus the corresponding IMF at intermediate and/or high mass could be steeper than the IMF in a typical young cluster if the low mass stars systematically drift further from their points of origin than higher mass stars.

In the case of the LMC even though the field IMF is observed to be steep, it could still originate from the same shallow IMF observed in stellar systems after they disperse. Differential evaporation of stars from the periphery of dispersed stellar systems or differential drift of long-lived low-mass stars into the field are expected to steepen the field IMF (e.g. Elmegreen 1997). An example of such a process has been presented by Gouliermis et al. (2002), who found a clear difference between the IMF slope of association LH 95 in the LMC, its surrounding field and the general field of the galaxy for the same mass range ($3 \lesssim M/M_\odot \lesssim 10$), with the IMF becoming gradually steeper outwards from the main body of the association. They interprete this phenomenon as due to the evaporation of the dispersed association, which feeds the general LMC field with intermediate-mass stars through its surrounding field, while the system itself is characterized by a centrally concentrated clump of massive stars, as if mass segregation takes place. Intermediate-mass stars ($\lesssim 15\,M_\odot$) in the outer parts of mass segregated young LMC clusters have steep IMF with slopes $\Gamma \lesssim -2$ (de Grijs et al. 2002a; Gouliermis et al. 2004). Whether this kind of stars in associations have the time to migrate and produce the observed steep field IMF is an open issue.

In any case Elmegreen (1999) notes that either the IMF is independent of star-forming density, and the general LMC field is somehow not a representative sample, or there is a threshold low density where the IMF abruptly changes from Salpeter-like to something much steeper at lower density. He proposes a field IMF that is a superposition of IMFs from many star-forming clouds, all with different masses, and he assumes that the largest stellar mass in each cloud increases with the cloud mass, perhaps because it takes a more massive star to destroy a more massive cloud. He suggests that since many clouds, even small ones, can produce low mass stars, but only the larger clouds produce high mass stars, the summed IMF will be steeper than the individual cloud IMF. However, his previously developed model for the stellar IMF (Elmegreen 1997), which is based on random selection of gas pieces in a hierarchical cloud, with a selection probability proportional to the square root of density and a lower mass cutoff from the lack of self-gravity, cannot explain the steep slope of the extreme field IMF without considering *significantly different physical effects*.

More recently, Elmegreen (2004) introduced a multicomponent IMF model, where he discusses three characteristic masses and their possible origins. He presents two examples where different parts of the IMF are relatively independent to demonstrate that the observed power law distributions ranging from solar-mass to high-mass stars *do not necessarily imply a single scale-free star formation mechanism, but the IMF can be a composite of IMFs from several different physical processes*. Brown dwarfs with masses of the order of $0.02\,M_\odot$ may be the result of dynamical processes inside self-gravitating pre-stellar condensations or gravitational collapse

in the ultra high-pressure shocks between these condensations. Solar-to-intermediate mass stars could be formed from the pre-stellar condensations themselves, getting their characteristic mass from the thermal Jeans mass in the cloud core. High-mass stars could grow from enhanced gas accretion and coalescence of pre-stellar condensations. These processes, blended together or with poor sampling statistics, can produce what appears to be a universal IMF. But when IMF is viewed with good statistics (like in our case here) on small scales and for specific mass ranges a diversity shows up, which can be interpreted as a variable IMF. According to Elmegreen (2004) these processes, which may as well coexist for all three considered mass ranges, broaden each component in his IMF models into what was approximated as a log-normal.

New results from HST/WFPC2 observations on the low-mass MF in the LMC, were recently provided by Gouliermis et al. (2005). Two areas in the LMC were studied, one on the stellar association named LH 52 (Lucke & Hodge 1970) and one on the background field of the close-by association LH 55. It was found that the low-mass MF slope of the field in the LMC, is independent of the location (an empty general field or the area of a star forming association) and it has a value between $-4 \gtrsim \Gamma \gtrsim -6$ for stars with masses $1 \lesssim M/M_{\odot} \lesssim 2$. In Gouliermis et al. (2005) the data did not contain information on the MF slope for lower masses, while in the present study we are able to get this information and we find statistically significant evidence that the MF becomes shallower for $M \lesssim 1\,M_{\odot}$.

The investigation on the general field of the LMC by Massey et al. (1995) gave IMF slopes, for stars $M \gtrsim 2\,M_{\odot}$, which have more or less the same slope as we found for $1 \lesssim M/M_{\odot} \lesssim 2$. This result clearly implies that the IMF slope of the LMC field is much steeper than Salpeter's, for the whole so far observed mass range with $M \gtrsim 1\,M_{\odot}$. Furthermore, Chabrier (2003) in an extensive review derives MF slopes for the Galactic field. We find that the slopes of the IMF of our observed LMC field, given in Table 2, are comparable to the ones by Chabrier for stars with $M \gtrsim 1\,M_{\odot}$.

This paper is based on observations made with the NASA/ESA Hubble Space Telescope, obtained from the data archive at the Space Telescope Science Institute. STScI is operated by the Association of Universities for Research in Astronomy, Inc. under NASA contract NAS 5-26555. This research has made use of NASA's Astrophysics Data System Bibliographic Services (ADS), of the SIMBAD database, operated at CDS, Strasbourg, France, and of *Aladin* (Bonnarel et al. 2000).

REFERENCES

Alexander, D. R., Brocato, E., Cassisi, S., Castellani, V., Ciacio, F., & degl'Innocenti, S. 1997, A&A, 317, 90
Andersen, J. 1991, A&AR, 3, 91
Baraffe, I., Chabrier G., Allard, F., & Hauschildt, P. H. 1995, ApJ, 446, L35
Barrado y Navascués, D., Stauffer, J. R., Bouvier, J., Martín, E. L. 2001, ApJ, 546, 1006
Basu, S. & Jones, C. E. 2004, MNRAS, 347, L47
Bate, M. R., Bonnell, I. A. & Bromm, V. 2002, MNRAS, 332, L65
Bonnarel, F., et al. 2000, A&AS, 143, 33
Bonnell, I. A., & Davies, M. B. 1998, MNRAS, 295, 691
Bonnell, I. A., Bate, M. R., & Zinnecker, H. 1998, MNRAS, 298, 93
Bonnell, I. A., Clarke, C. J., Bate, M. R. & Pringle, J. E. 2001, MNRAS, 324, 573
Bonnell, I. A., Bate, M. R., & Vine, S. G. 2003, MNRAS, 343, 413
Bonnell, I. A., Vine, S. G., & Bate, M. R. 2004, MNRAS, 349, 735
Bouvier, J., Stauffer, J. R., Martin, E. L., Barrado y Navascués, D., Wallace, B., & Bejar, V. J. S. 1998, A&A, 336, 490
Briceño, C., Luhman, K. L., Hartmann, L., Stauffer, J. R., & Kirkpatrick, J. D. 2002, ApJ, 580, 317
Brown, A. G. A. 1998, ASP Conf. Ser. 142: The Stellar Initial Mass Function (38th Herstmonceux Conference), 142, 45
Casassus, S., Bronfman, L., May, J., Nyman, L.-Å 2000, A&A, 358, 514
Castro, R., Santiago, B. X., Gilmore, G. F., Beaulieu, S., & Johnson, R. A. 2001, MNRAS, 326, 333
Chabrier, G. 2003, PASP, 115, 763
Chabrier, G., Baraffe, I., & Plez, B. 1996, ApJ, 459, L91
Cheselka, M., Holberg, J. B., Watkins, R., & Collins, J. 1993, AJ, 106, 2365
Churchwell, E. 2002, ARAA, 40, 27
de Grijs, R., Gilmore, G. F., Johnson, R. A., & Mackey, A. D. 2002a, MNRAS, 331, 245
de Grijs et al. 2002b, MNRAS, 337, 597
Delgado-Donate, E.J., Clarke, C.J., & Bate, M.R. 2004, MNRAS, 347, 759
Dolphin, A. E. 2000a, PASP, 112, 1383
Dolphin, A. E. 2000b, PASP, 112, 1397
Dolphin, A. E. & Hunter, D. A. 1998, AJ, 116, 1275
Elmegreen, B. G. 1997, ApJ, 486, 944
Elmegreen, B. G. 1998, ASP Conf. Ser. 148: Origins, 148, 150
Elmegreen, B.G. 1999, ApJ, 515, 323
Elmegreen, B. G. 2004, MNRAS, 354, 367
Elson, R. A. W., Gilmore, G. F., & Santiago, B. X. 1997, MNRAS, 289, 157
Elson, R. A. W., Sigurdsson, S., Hurley, J., Davies, M. B., & Gilmore, G. F. 1998, ApJ, 499, L53
Fischer, Ph., Pryor, C., Murray, S., Mateo, M., & Richtler, T. 1998, AJ, 115, 592
Gallagher, J. S., Mould, J. R., de Feijter, E., et al. 1996, ApJ, 466, 732
Gammie, C. F., Lin, Y.-T., Stone, J. M., & Ostriker, E. C. 2003, ApJ, 592, 203
Garay, G., Lizano, S. 1999, PASP, 111, 1049
García-Berro, E., Ritossa, C., & Iben, I., Jr. 1997, ApJ, 485, 765
Garmany, C. D., Conti, P. S., & Chiosi, C. 1982, ApJ, 263, 77
Garmany, C. D., Massey, Ph., & Parker, J. W. 1994, AJ, 108, 1256
Geha, M. C., et al. 1998, AJ, 115, 1045
Gerhard, O. 2000, ASP Conf. Ser. 211: Massive Stellar Clusters, 211, 12
Giersz, M., Heggie, D. C. 1996, MNRAS, 279, 1037
Girardi, L., Bressan, A., Bertelli, G., & Chiosi, C. 2000, A&AS, 141, 371
Girardi, L., Bertelli, G., Bressan, A., et al. 2002, A&A, 391, 195
Gouliermis, D., et al. 2002, A&A, 381, 862
Gouliermis, D., Keller, S. C., Kontizas, M., Kontizas, E., & Bellas-Velidis, I. 2004, A&A, 416, 137
Gouliermis, D., Brandner, W., & Henning, T. 2005, ApJ, 623, 846
Grebel, E. K., & Chu, Y.-H. 2000, AJ, 119, 787
Henry, T. J., & McCarthy, D. W. 1993, AJ, 106, 773
Hill, J. K., et al. 1994, ApJ, 425, 122
Hill, R. S., et al. 1995, ApJ, 446, 622
Hillenbrand, L. A. & Carpenter, J. M. 2000, ApJ, 540, 236
Holtzmann, J., A., Burrows, C., Casertano, S., Hester, J., Trauger, J., Watson, A., & Worthey, G. 1995, PASP, 107, 1065
Holtzman, J. A., et al. 1999, AJ, 118, 2262
Hunter, D. A., et al. 1997, ApJ, 478, 124
Javiel, S. C., Santiago, B. X., & Kerber, L. O. 2005, A&A, 431, 73
Jeffries, R. D. 1997, MNRAS, 288, 585
Kontizas, M., Morgan, D. H., Hatzidimitriou, D., & Kontizas, E. 1990, A&AS, 84, 527
Kontizas, M., Kontizas, E., & Michalitsianos, A. G. 1993, A&A, 269, 107
Koornneef, J. 1983, A&A, 128, 84
Kroupa, P. 2002, Science, 295, 82
Kroupa, P., Tout, C. A., & Gilmore, G. 1990, MNRAS, 244, 76 (KTG90)
Kroupa, P., Tout, C. A., & Gilmore, G. 1993, MNRAS, 262, 545
Kroupa, P., & Tout, C. A. 1997, MNRAS, 287, 402
Kroupa, P., Aarseth, S., & Hurley, J. 2001, MNRAS, 321, 699
Kroupa, P., & Bouvier, J. 2003, MNRAS, 346, 369
Kroupa, P., & Weidner, C. 2003, ApJ, 598, 1076
Lada, E. A., Lada, C. J., & Muench, A. 1998, ASP Conf. Ser. 142: The Stellar Initial Mass Function (38th Herstmonceux Conference), 107
Larson, R. B. 1990, ASSL Vol. 162: Physical Processes in Fragmentation and Star Formation, 389
Larson, R. B. 1999, Star Formation 1999, Proceedings of Star Formation 1999, held in Nagoya, Japan, June 21 - 25, 1999, Editor: T. Nakamoto, Nobeyama Radio Observatory, p. 336-340
Larson, R. B. 2002, MNRAS, 332, 155
Le Duigou, J.-M., Knödlseder, J. 2002, A&A, 392, 869
Leitherer, C. 1998, ASP Conf. Ser. 142: The Stellar Initial Mass Function (38th Herstmonceux Conference), 142, 61
Leitherer, C. & Wolf, B. 1984, A&A, 132, 151
Li, Y., Klessen, R. S., Mac Low, M. -M. 2003, ApJ 592, 975
Lucke, P. B. & Hodge, P. W. 1970, AJ, 75, 171
Luhman, K. L. 2000, ApJ, 544, 1044
Luhman, K. L., et al. 2000, ApJ, 540, 1016
Luhman, K. L., et al. 2003, ApJ, 593, 1093

Lyo, A. -R., Lawson, W. A., Feigelson, E. D., & Crause, L. A. 2004, MNRAS, 347, 246
Malkov, O. & Zinnecker, H. 2001, MNRAS, 321, 149
Massey, P. 1998, ASP Conf. Ser. 142: The Stellar Initial Mass Function (38th Herstmonceux Conference), 142, 17
Massey, P. 2002, ApJS, 141, 81
Massey P., Silkey M., Garmany C.D., Degioia-Eastwood K., 1989a, AJ, 97, 107
Massey P. Parker J.W., Garmany C.D. 1989b, AJ, 98, 1305
Massey, Ph., Lang, C. C., Degioia-Eastwood, K. & Garmany, C. D. 1995, ApJ, 438, 188
Massey, P. & Hunter, D. A. 1998, ApJ, 493, 180
McKee, C. F. & Tan, J. C. 2003, ApJ, 585, 850
Metcalfe, N., Shanks, T., Campos, A., McCracken, H. J., & Fong, R. 2001, MNRAS, 323, 795
Mihalas, D. & Binney, J. 1981, Galactic Astronomy (San Francisco: Freeman)
Miller, G. E., & Scalo, J. M. 1979, ApJS, 41, 513
Muench, A. A., Lada, E. A., Lada, C. J., & Alves, J. 2002, ApJ, 573, 366
Muench, A. A., et al. 2003, AJ, 125, 2029
Myers, P. C. 2000, ApJ, 530, L119
Oey, M. S. 1996, ApJ, 465, 231
Oey, M. S., & Massey, P. 1995, ApJ, 452, 210
Olsen, K. A. G., Kim, S., & Buss, J. F. 2001, AJ, 121, 3075
Padoan, P., & Nordlund, Å. 2002, ApJ, 576, 870
Panagia, N., Gilmozzi, R., Macchetto, F., Adorf, H.-M., & Kirshner, R. P. 1991, ApJL, 380, L23
Parker, J. W., Garmany, C. D., Massey, P., & Walborn, N. R. 1992, AJ, 103, 1205
Parker, J. W., et al. 1998, AJ, 116, 180
Parker, J. W., Zaritsky, D., Stecher, T. P., Harris, J., & Massey, P. 2001, AJ, 121, 891
Piotto, G., Cool, A. M., & King, I. R. 1997, AJ, 113, 1345
Pols, O. R., Schroder, K., Hurley, J. R., Tout, C. A., & Eggleton, P. P. 1998, MNRAS, 298, 525
Portegies-Zwart, Simon F., Baumgardt, H., Hut, P., Makino, J., McMillan, S. L. W. 2004, Nature, 428, 724
Preibisch, T., Stanke, T. & Zinnecker, H. 2003, A&A, 409, 147
Press, W. H., Teukolsky, S. A., Vetterling, W. T., & Flannery, B. P. 1992, "Numerical recipes in FORTRAN. The art of scientific computing", Cambridge: University Press, 2nd ed.
Price, N. M., & Podsiadlowski, Ph. 1995, MNRAS, 273, 104
Rana, N. C. 1987, A&A, 184, 104
Ratnatunga, K. U. & Bahcall, J. N. 1985, ApJS, 59, 63
Reid, N. 1998, ASP Conf. Ser. 142: The Stellar Initial Mass Function (38th Herstmonceux Conference), 142, 121
Reid, N., et al. 1999, ApJ, 521, 613
Reipurth, B. & Clarke, C. 2001, AJ, 122, 432
Rieke, G. H., & Lebofsky, M. J. 1985, ApJ, 288, 618
Salasnich, B., Girardi, L., Weiss, A., & Chiosi, C. 2000, A&A, 361, 1023
Salpeter, E. E. 1955, ApJ, 121, 161
Scalo, J. 1986, Fundam. Cosmic Phys., 11, 1
Scalo, J. 1990, ASSL Vol. 160: Windows on Galaxies, 125
Scalo, J. 1998, ASP Conf. Ser. 142: The Stellar Initial Mass Function (38th Herstmonceux Conference), 201
Sirianni, M., Nota, A., De Marchi, G., Leitherer, C., Clampin, M. 2002, ApJ, 579, 275
Shadmehri, M. 2004, MNRAS, 354, 375
Smecker-Hane, T. A., Cole, A. A., Gallagher, J. S., & Stetson, P. B. 2002, ApJ, 566, 239
Stahler, S. W., Palla, F., & Ho., P. T. P. 2000, Protostars and Planets IV, 327
Stobie, R. S., Ishida, K., & Peacock, J. A. 1989, MNRAS, 238, 709
Stolte, A., Grebel, E. K., Brandner, W. & Figer, D. F. 2002, A&A, 394, 459
Taylor, B. J. 1986, ApJS, 60, 577
Tsujimoto, T., Yoshii, Y., Nomoto, K., Matteucci, F., Thielemann, F.-K., & Hashimoto, M. 1997, ApJ, 483, 228
Weidemann, V. 1990, ARA&A, 28, 103
Wood, M. A. 1991, in Proc. Ninth European Workshop on White Dwarfs, ed. D. Doester & K. Werner (Berlin: Springer), 612
Yorke, H. W. Sonnhalter, C. 2002, ApJ, 569, 846
Zinnecker, H. 1982, New York Academy Sciences Annals, 395, 226
Zinnecker, H. 1986, IAU Symp. 116: Luminous Stars and Associations in Galaxies, 116, 271
Zinnecker, H. 1996, The Interplay Between Massive Star Formation, the ISM and Galaxy Evolution, 249